EPJ Web of Conferences **138**, 01019 (2017) DOI: 10.1051/epjconf/201713801019
Baldin ISHEPP XXIII

Comparative analysis of the pion-nucleus scattering within the microscopic Folding and the local Kisslinger type potentials

Valery Lukyanov[1,⋆] *Elena* Zemlyanaya[1], *Konstantin* Lukyanov[1], and *Ibrahim* Abdul-Magead[2]

[1] *Joint Institute for Nuclear Research, Dubna, Russia*
[2] *Cairo University, Giza, Cairo, Egypt*

Abstract. Elastic scattering cross sections are calculated and compared to the data of $\pi^{\pm}$ + ^{28}Si and ^{40}Ca at energies 130, 180, and 230 MeV by using the both microscopic optical potentials (OP), the high-energy folding and the local Kisslinger type potentials. In the folding OP, we use the known nuclear density distributions while parameters of the elementary πN-scattering amplitude are fitted to the data with the aim to estimate the in-medium effect on pions scattered on bound nucleons. As to the local modified Kisslinger OP its parameters are known from the earlier studies. The cross sections for both OPs are calculated by solving the Klein-Gordon wave equation, and thus the relativistic and distortion effects on the process are accounted for exactly. A fairly well agreement with experimental data was obtained and the decisive role of a surface region of potentials was established where both OPs occur in close coincidence.

1 Introduction

In our theoretical study of π-nucleus scattering we apply two models. In *the first* one we use the optical potential (OP) from [1] where it was obtained as the local OP in a wave equation for the $\psi(r)$-function after the Krell-Ericson transformation [2] of the ordinary $\phi(r)$ wave function of an ordinary wave equation with the non-local Kisslinger OP $U = a(r) + \nabla b(r)\nabla$ [3]. The 12 parameters of this local OP were obtained in [1] by fitting the calculated π-A differential cross section to the data measured at energies in the region of the 3-3 pion-nucleon resonance. These $\phi(r)$ and $\psi(r)$ functions are shown to be phase equivalent solutions of the respective wave equations. *The second model* of OP [4] corresponds to the eikonal phase of the Glauber high-energy approximation [5] and, in fact, becomes the folding integral of the πN amplitude and form factor of the nuclear density distribution function. For the pion-nucleus scattering this OP was applied in [6], and unlike the Glauber approach for the scattering amplitude where one uses integration along the straight line trajectory of motion, in our calculations we solve the Klein-Gordon relativistic wave equation and thus relativistic and distortion effects are accounted for exactly. For both OPs, we compare the calculated differential cross sections with experimental data and thus obtain forms of respective potentials to establish the meaningful regions of nuclei that reveal themselves in the pion scattering.

The aims of our study are to explain the experimental data in the region of πN 3-3-resonance energies, to compare the calculated cross sections for both models, and to estimate the "in-medium"

⋆e-mail: vlukyanov@theor.jinr.ru

effect on the elementary πN scattering amplitude. The parameters of the latter are obtained by fitting the calculated πA differential cross sections to the respective experimental data on elastic scattering. The established best-fit "in-medium" πN parameters are compared with those for the corresponding "free" πN scattering amplitudes. Application is presented for elastic scattering of pions on nuclei ^{28}Si and ^{40}Ca at energies 130, 180, and 230 MeV.

2 Basic equations

The microscopic folding OP is taken as done in [4]

$$U(r) = -\frac{(\hbar c)\beta_c}{2(2\pi)^3}\,\sigma\,[i+\alpha]\cdot\int e^{-i\mathbf{qr}}\rho(q)\,f(q)\,d^3q, \tag{1}$$

where β_c is the speed of light, $f(q)$ – form factor of the πN-amplitude $F_{\pi N}(q)$, and $\rho(q)$ is the form factor of a nuclear density distribution

$$\rho(q) = \int e^{i\mathbf{qr}}\,\rho(r)\,d^3r. \tag{2}$$

Here we use the charge-independent principle which enables one to apply the averaged πN-amplitude

$$F_{\pi N}(q) = \frac{k}{4\pi}\,\sigma\,[i+\alpha]\cdot f(q), \qquad f(q) = e^{-\beta q^2/2}, \tag{3}$$

dependent on 3 parameters instead of 12 parameters needed for the separate $\pi^{\pm}p$- and $\pi^{\pm}n$- amplitudes. So, σ is the total cross section, α, the ratio of real to imaginary part of the amplitude at forward angles, and β, the slope parameter. In calculations of the folding OP (1) we take the nuclear density distribution $\rho(r)$ in the form of a symmetrized Fermi-function, for which the form factor $\rho(q)$ can be presented in an analytic form, and thus

$$\rho_{SF}(r) = \rho_0\frac{\sinh(R/a)}{\cosh(R/a)+\cosh(r/a)}, \quad \rho_0 = \frac{A}{1.25\pi R^3}\Big[1+(\frac{\pi a}{R})^2\Big]^{-1}, \tag{4}$$

$$\rho_{SF}(q) = -\rho_0\,\frac{4\pi^2 aR}{q}\,\frac{\cos qR}{\sinh(\pi aq)}\left[1-\left(\frac{\pi a}{R}\right)\coth(\pi aq)\tan qR\right]. \tag{5}$$

In our applications of the folding optical potential (1), the radius R and diffuseness parameters a of the target nuclei ^{32}Si and ^{40}Ca are taken from the respective electron-nucleus scattering data. In the case of the folding potential (1), when comparing calculated cross sections to experimental data we will fit three parameters σ, α, and β, and thus the obtained magnitudes of them will characterize the amplitude of scattering of pions on the bound nucleons, i.e. the so-called "in-medium" effect.

As to *the local model of Kisslinger − type OP* developed in [1] it was realized in the form

$$U(r) = \frac{(\hbar c)^2}{2E}\,\frac{1}{1-\alpha(r)}\Big\{q(r)-k^2\alpha(r)-(1/2)\nabla^2\alpha\Big[1+\frac{(1/2)\nabla^2\alpha}{1-\alpha}\Big]\Big\}, \tag{6}$$

where the first term arises from the s- and p-wave πN interaction, while the other smaller terms are from the p-wave alone, and

$$q(r) = -4\pi[\mathbf{b_0}\rho(r)\mp\mathbf{b_1}\Delta\rho(r)]/p_1+\delta q, \tag{7}$$

$$\alpha(r) = 4\pi[\mathbf{c_0}\rho(r)\mp\mathbf{c_1}\Delta\rho(r)]/p_1+4\pi[\mathbf{C_0}\rho^2(r)\mp\mathbf{C_1}\rho(r)\Delta\rho(r)]/p_2, \tag{8}$$

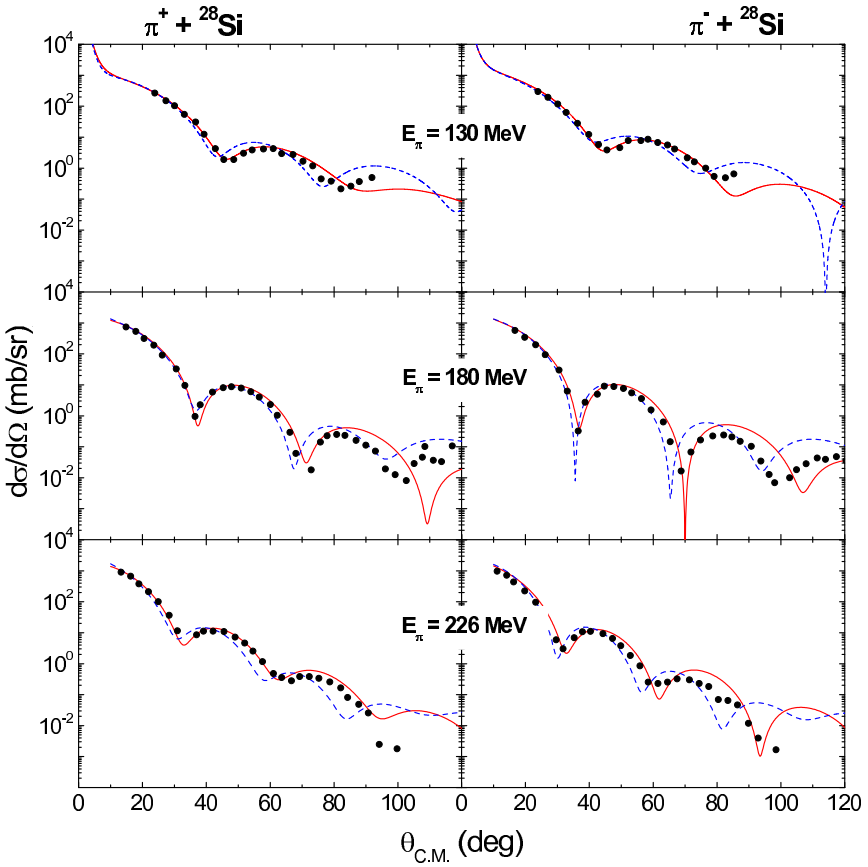

Figure 1. Comparisons of the calculated $\pi^{\pm} + {}^{28}Si$ elastic scattering cross sections at the pion energies 130, 180, and 230 MeV with experimental data from [7]. Solid (red) curves correspond to the folding OP, and dashed (blue) curves are for the local Kisslinger-type OP. The best fit "in-medium" parameters σ, α, β of the πN scattering amplitude are from table 1.

$$\delta q(r) = -2\pi\epsilon\nabla^2\{[\mathbf{c_0}\rho(r) \mp \mathbf{c_1}\Delta\rho(r)]/p_1 + \frac{1}{2}[\mathbf{C_0}\rho^2(r) \mp \mathbf{C_1}\rho(r)\Delta\rho(r)]/p_2]\}. \quad (9)$$

Here $\mathbf{b_{0,1}}$, $\mathbf{c_{0,1}}$, $\mathbf{C_{0,1}}$ are the complex parameters fitted, e.g. in [1] as functions of an energy. Then, E is the total pion energy in c.m system, $p_1 = 1 + \epsilon$, $p_2 = 1 + (1/2)\epsilon$ with $\epsilon = E/Mc^2$ and Mc^2 the nucleon mass.

The differential cross sections are calculated as done in [8] by solving the Klein-Gordon equation in its form at conditions $E \gg U$ (below $\hbar = c = 1$)

$$\left(\Delta + k^2\right)\psi(\vec{r}) = 2\bar{\mu}U(r)\psi(\vec{r}), \quad U(r) = U^H(r) + U_C(r). \quad (10)$$

Here k is the relativistic momentum of pions in center-of-mass (c.m.) system,

$$k = \frac{M_A k^{lab}}{\sqrt{(M_A + m_\pi)^2 + 2M_A T^{lab}}}, \quad k^{lab} = \sqrt{T^{lab}\,(T^{lab} + 2m_\pi)}, \quad (11)$$

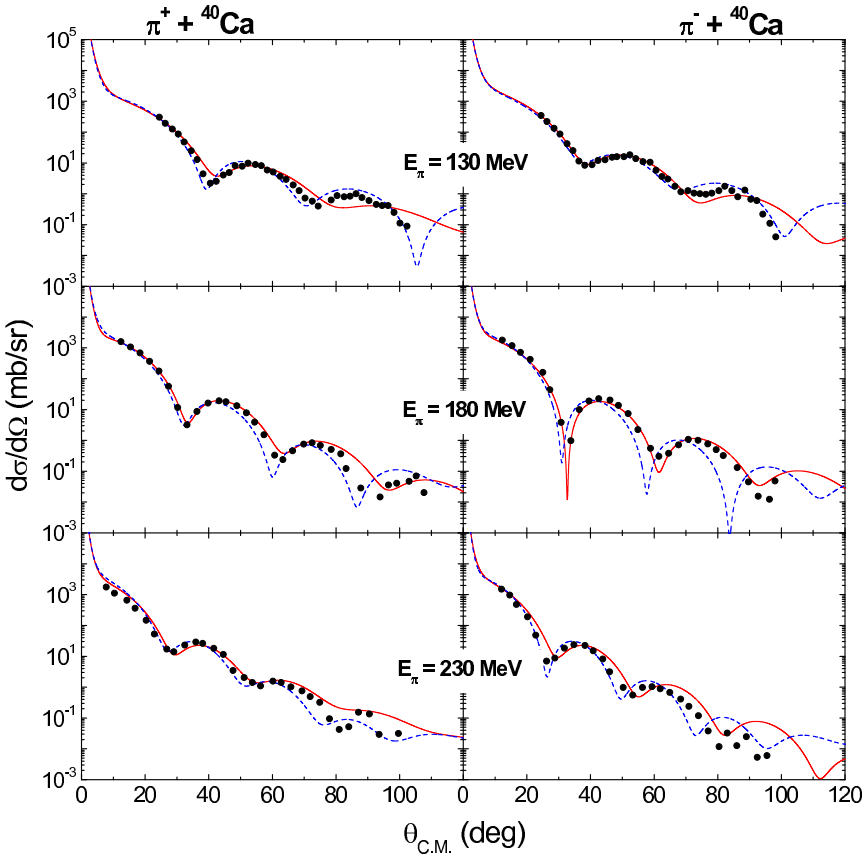

Figure 2. The same as in figure 1 but for the elastic scattering of $\pi^{\pm} + {}^{40}Ca$. Experimental data are from [9].

and $\bar{\mu} = \frac{EM_A}{E+M_A}$ is the relativistic reduced mass, $E = \sqrt{k^2 + m_\pi^2}$ – total energy, m_π and M_A are the pion and nucleus masses.

In the case of the folding potential (1), when comparing calculated pion-nucleus cross sections to experimental data, the fitted parameters σ, α, and β have a meaning of the so-called "in-medium" parameters for the amplitude of scattering of pions on the bound nucleons. The fitting procedure of their minimization was realized in [10] and [11] for the χ^2-function

$$\chi^2 = f(\sigma,\alpha,\beta) = \sum_i \frac{(y_i - \hat{y}_i(\sigma,\alpha,\beta))^2}{s_i^2}, \tag{12}$$

where $y_i = \dfrac{d\sigma}{d\Omega}$ and $\hat{y}_i = \dfrac{d\sigma}{d\Omega}(\sigma,\alpha,\beta)$ are, respectively, experimental and theoretical differential cross sections, s_i are experimental errors.

3 Results of calculations

Figures 1 and 2 demonstrate a reasonable agreement of the calculated and experimental differential cross sections of elastic scattering of $\pi^{\pm}$-mesons on nuclei ${}^{32}Si$ and ${}^{40}Ca$ at energies 130, 180, and

Table 1. The best-fit parameters σ, α, β and respective χ^2/k quantities with k, the number of experimental points at $\Theta_{C.M.}$ between 0 and 80 degrees ([10]).

reaction	T^{lab}, MeV	σ, fm^2	α	β, fm^2	χ^2/k
π^-+^{28}Si	130	7.22	0.84	0.78	0.9
π^++^{28}Si		9.59	0.11	0.83	2.7
π^-+^{40}Ca		6.86	0.90	0.88	3.9
π^++^{40}Ca		8.21	0.10	0.76	14.4
π^-+^{28}Si	180	9.33	0.43	0.28	6.0
π^++^{28}Si		7.75	0.76	0.49	1.2
π^-+^{40}Ca		9.75	0.21	0.27	3.0
π^++^{40}Ca		5.75	1.09	0.69	2.9
π^-+^{28}Si	226	7.43	0.60	0.17	16.2
π^++^{28}Si		9.99	-0.13	0.12	21.5
π^-+^{40}Ca	230	5.34	0.79	0.23	6.4
π^++^{40}Ca		9.17	-0.10	0.24	9.6

230 MeV. Experimental data are taken from [7] and [9]. In the case of folding OP (solid red curves) we used the nuclear point-density-distributions (for centers of nucleons) in the form of a symmetrized fermi-function (4) with the radius R and diffuseness a parameters $R = 3.134$ fm and $a = 0.477$ fm for ^{28}Si, and $R = 3.593$ fm and $a = 0.493$ fm for ^{40}Ca (see [12]). As to the"in-medium" parameters σ, α, β of a πN scattering amplitude they have been fitted in [10] and [11], and the corresponding χ^2 magnitudes per one experimental point are presented in table 1 for the region of scattering angles up to 80 degrees. The "in-medium" effect is revealed more clearly when one compares the"in-medium" parameters to the respective parameters for the pion scattering on "free" nucleons done in [13]. Thus, to express the "in-medium" effect more markedly we show in figure 3 the differences of corresponding "in-medium" and "free" parameters as shadowed regions by blue color.

As for the cross sections calculated within the local Kisslinger-type optical potentials, they are shown in Figures 1 and 2 by dotted blue curves. The respective 12 parameters of OPs have already been fitted in [1] in dependence of an energy, and the full nuclear density parameters in the form of a symmetrized fermi-function (4) were taken as $R = 3.134$ fm and $a = 0.537$ fm for ^{28}Si from [14], and $R = 3.53$ fm and $a = 0.562$ fm for ^{40}Ca .Their applications for our case lead to about the same χ^2 magnitudes that were obtained for the folding OPs. Thus one can conclude that in spite of

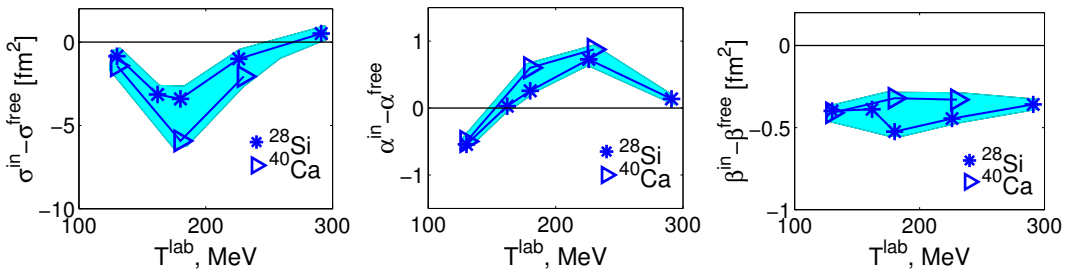

Figure 3. The behavior of differences of the fitted "in-medium" and "free" parameters of the πN scattering amplitude (3) at the energy region of 3-3-resonance.

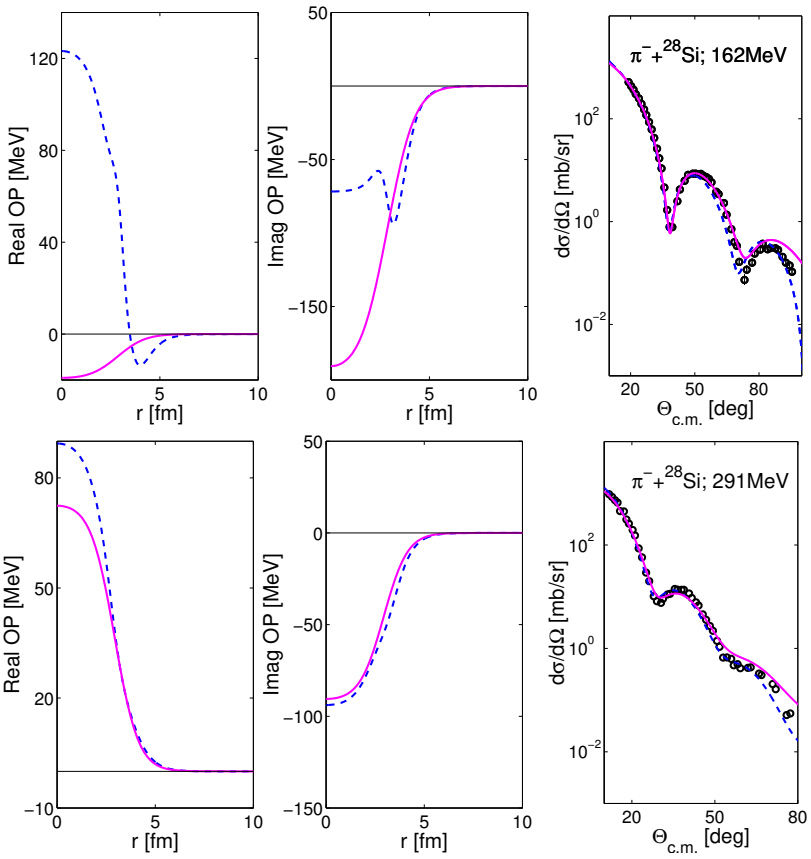

Figure 4. Comparisons of the folding (solid, red curves) and local Kisslinger-type (dashed, blue) optical potentials, and the corresponding cross sections for π^+-^{28}S scattering at T_{lab}=162 and 291 Mev.

the so different constructions of employed potentials and sometimes different behavior of them as function of r, both OPs yield cross sections in reasonably good agreement with the experimental data at energies of 3-3 resonance. However this does not mean that the forms of both OPs should be close to each other. Indeed, as an example, in figure 4 we show the optical potentials and corresponding cross sections at different energies 162 and 291 MeV for the π^- scattering on ^{32}Si. One can see that for each energy the calculated cross sections for both OPs are in a good coincidence. At the same time, at lower energy 162 MeV the real part of a local Kisslinger-type potential is repulsive in the inner part of a nucleus, while its imaginary part is negative and almost coincides to the folding OP in a surface region. On the other hand, at higher energy 291 MeV both OPs have similar forms for both real and imaginary parts, and have no any variations as function of r. So, one can conclude that behavior of the imaginary part of OP in its surface region plays a decisive role in explanation of experimental data at the first quarter of angles.

4 Summary

One can sum up that our approach based on 3-parameter OP, allows one to explain fairly well the experimental data on pion-nucleus elastic scattering. Moreover, we show that both microscopic folding and local Kisslinger-type optical potentials provide a good agreement with the experimental data of pion-nucleus elastic scattering at intermediate energies in the region of the πN 3-3 resonance between 130 and 230 MeV. Such an agreement takes place in spite of the fact that the Kisslinger-type potential has some variations in its inner part. At the same time both potentials are close to each other in the surface region and thus one can conclude that this region plays a decisive role in the mechanism of scattering. Comparisons of the πN cross section σ^{free} with σ^{in} at 3-3-resonance region show that the pion interaction with bound nucleons in nuclear matter is weaker than in the case of free nucleons. The behavior of the parameter α indicates that the refraction process increases at larger energies $T^{lab} \geq 170$ MeV.

In general, when modeling the elastic scattering data alone we face the ambiguity problem when several approaches explain the same amount of data. For example, in [15] just the same data as applied in figures 1,2 have been successfully explained basing on the optical potential that corresponds to the first and second order parts of multiple scattering theory and fitting the phenomenological ρ^2-dependent term added to account for, say, the pion collisions with the couples of nucleons in nuclei. In this connection, the data on inelastic πA-scattering may help us to reduce this ambiguity. Indeed, in the models of such processes one applies the derivative of the already fitted elastic scattering OP, that reveals itself mainly in the surface region. So, in [16] the data on the inelastic scattering cross sections with excitations of 2^+ and 3^- collective states of nuclei were explained fairly well basing on the known folding OPs and on the only additional parameter, the deformation of a nuclear surface.

References

[1] M.B. Johnson and G.R. Satchler, Ann. Phys. **248**, 134 (1996)
[2] M. Krell and T.E.O. Ericson, Nucl. Phys. B **11**, 521 (1969)
[3] L.S. Kisslinger, Phys. Rev. **98**, 761 (1955)
[4] V.K. Lukyanov, E.V. Zemlyanaya, K.V. Lukyanov, Phys. Atom. Nucl. **69**, 240 (2006)
[5] R.J. Glauber, *Lectures in Theoretical Physics* (Interscience, New York, 1959) 315
[6] V.K. Lukyanov, E.V. Zemlyanaya, K.V. Lukyanov, Phys. Atom. Nucl. **77**, 100 (2014)
[7] B.M. Preedom et al., Nucl. Phys. A **326**, 385 (1979)
[8] V.K. Lukyanov, E.V. Zemlyanaya, K.V. Lukyanov, K.M. Hanna, Phys. Atom. Nucl. **73**, 1443 (2010)
[9] P. Gretillat et al., Nucl. Phys. A **364**, 270 (1981)
[10] V.K. Lukyanov, E.V. Zemlyanaya, K.V. Lukyanov, E.I. Zhabitskaya, M.V. Zhabitsky, Preprint JINR P4-2012-105, Dubna, 2012
[11] V.K. Lukyanov, E.V. Zemlyanaya, K.V. Lukyanov, E.I. Zhabitskaya, M.V. Zhabitsky, Phys. Atom. Nucl. **77**, 100 (2014)
[12] V.K. Lukyanov, E.V. Zemlyanaya, B. Słowinski, Phys. Atom. Nucl. **67**, 1282 (2004)
[13] M.P. Locher, O. Steinmann, N. Straumann, Nucl. Phys. B **27**, 598 (1971)
[14] H. De Vries, C.W. De Jager, C. De Vries, Atomic Data and Nucl. Data Tables **36**, 495 (1987). Nucl. Phys. B **27**, 598 (1971)
[15] M. Gmitro, S.S. Kamalov, R. Mach, Phys. Rev. **36**, 1105 (1987)
[16] V.K. Lukyanov, E.V. Zemlyanaya, K.V. Lukyanov, I.A.M. Abdul-Magead, Phys. Atom. Nucl. **79**, 670 (2016)